Original Article

Evaluation of parietal pleural adhesion and invasion in subpleural lung cancer: value of B-mode ultrasound and contrast-enhanced ultrasound

Yuxin Zhang[1,2#], Zhanwei Zhang[1#], Haixing Liao[1#], Maohan Li[1], Cong Xu[3], Zechun Liang[1], Liantu He[1,2], Shiyu Zhang[1], Qing Tang[1,2]

[1]Department of Ultrasound, First Affiliated Hospital of Guangzhou Medical University, Guangzhou, China; [2]The State Key Laboratory of Respiratory Disease, Guangzhou Institute of Respiratory Disease, the First Affiliated Hospital, Guangzhou Medical University, Guangzhou, China; [3]Department of Medicine Ultrasonics, Nanfang Hospital, Southern Medical University, Guangzhou, China

Contributions: (I) Conception and design: Y Zhang, Z Zhang, S Zhang, Q Tang; (II) Administrative support: L He, H Liao, Q Tang; (III) Provision of study materials or patients: Z Zhang, S Zhang, C Xu; (IV) Collection and assembly of data: M Li, Z Liang; (V) Data analysis and interpretation: Y Zhang, Z Zhang, S Zhang, H Liao; (VI) Manuscript writing: All authors; (VII) Final approval of manuscript: All authors.

[#]These authors contributed equally to this work as co-first authors.

Correspondence to: Shiyu Zhang, MD. Department of Ultrasound, First Affiliated Hospital of Guangzhou Medical University, 151 Yanjiang Rd., Guangzhou 510120, China. Email: 1030988051@qq.com; Qing Tang, MD. Department of Ultrasound, First Affiliated Hospital of Guangzhou Medical University, 151 Yanjiang Rd., Guangzhou 510120, China; The State Key Laboratory of Respiratory Disease, Guangzhou Institute of Respiratory Disease, the First Affiliated Hospital, Guangzhou Medical University, Guangzhou, China. Email: tqgyyy@126.com.

Background: The parietal pleural adhesion/invasion of lung cancer can contribute substantially to poor prognosis and difficulty in surgery. The value of ultrasound in evaluating the parietal pleural adhesion or invasion (pleural adhesion/invasion) of lung cancer remains uncertain. This study investigated the value of B-mode ultrasound and contrast-enhanced ultrasound (CEUS) in diagnosing parietal pleural adhesion/invasion of subpleural lung cancer.

Methods: The study animals included 40 male New Zealand white rabbits. A rabbit subpleural lung cancer model was constructed by injecting VX2 tumor tissue under ultrasound guidance. In the 1–3 weeks after subpleural lesion formation, parietal pleural adhesion/invasion of the largest subpleural lesion was evaluated with B-mode ultrasound and CEUS by two sonographers. The parietal pleural adhesion/invasion was also determined using the gold standard method of findings from anatomical and pathological examination.

Results: Ultimately, 34 rabbits were subjected to complete ultrasonic evaluation. There were 20 and 14 cases with and without parietal pleural adhesion/invasion, respectively, as confirmed by anatomical and pathological evaluations. The diagnostic sensitivity, specificity, and accuracy of sonographer 1 using B-mode ultrasound were 50.0% [95% confidence interval (CI): 26.0–74.0%], 100%, and 70.6% (95% CI: 54.5–86.7%), respectively; for CEUS, they were 90.0% (95% CI: 75.6–100.0%), 100.0%, and 94.1% (95% CI: 85.8–100.0%), respectively. The diagnostic sensitivity, specificity, and accuracy of sonographer 2 using B-mode ultrasound were 45.0% (95% CI: 21.1–68.9%), 92.9% (95% CI: 77.5–100.0%), and 64.7% (95% CI: 47.8–81.6%), respectively; for CEUS, they were 85.0% (95% CI: 67.9–100.0%), 100.0%, and 91.2% (95% CI: 81.1–100.0%), respectively. The diagnostic accuracy of sonographer 1 was higher with CEUS than with B-mode ultrasound, but not significantly so (94.1% *vs.* 70.6%; P=0.08). The diagnostic accuracy of sonographer 2 was significantly higher with CEUS than with B-mode ultrasound (91.2% *vs.* 64.7%; P=0.03). The interrater reliability was higher for CEUS than for B-mode ultrasound (κ=0.941 *vs.* κ =0.717).

Conclusions: Based on an animal model, B-mode ultrasound and CEUS both exhibited good diagnostic

efficacy and interrater reliability in evaluating parietal pleural adhesion/invasion of subpleural lung cancer although CEUS outperformed B-mode ultrasound for both measures.

Keywords: Lung neoplasms; parietal pleural adhesion; ultrasonography; contrast-enhanced ultrasound (CEUS); diagnostic imaging

Submitted Oct 31, 2023. Accepted for publication Jan 21, 2024. Published online Apr 26, 2024.
doi: 10.21037/qims-23-1542
View this article at: https://dx.doi.org/10.21037/qims-23-1542

Introduction

Lung cancer is a common cause of cancer-related death worldwide (1). Accurate tumor-node-metastasis (TNM) staging is crucial for optimizing treatment programs and improving prognosis, with the degree of pleural invasion of peripheral lung cancer being an important indicator of T staging. Specifically, parietal pleural invasion, designated as pleural invasion 3 based on pleura status, is a factor that contributes to poor prognosis and serves as an important indicator for upgrade to stage T3 (2-5). In such cases, radical surgery, such as extrapleural or total resection, is usually required (6,7). Moreover, parietal pleural adhesion/invasion increases surgical difficulty. Chemotherapy regimens also depend on the pleural invasion stage of lung cancer (8,9). Hence, precise preoperative identification of parietal pleural invasion is essential.

Several noninvasive medical imaging techniques have been reported for identifying parietal pleural invasion, with computed tomography (CT) being the most commonly used for lung cancer (10-12). Recently, one study attempted to identify parietal pleural invasion or adhesion (invasion/adhesion) by assessing the abnormal regional motion of the lung surface via four-dimensional dynamic-ventilation CT. The diagnostic accuracy for evaluating parietal pleural invasion or adhesion was significantly higher than that of conventional chest CT, although only 18 cases were investigated (10). Similarly, others have reported that dynamic magnetic resonance imaging (MRI) can help evaluate parietal pleural and chest wall invasion and improve conventional CT or MRI accuracy in predicting chest wall invasion of lung cancer (11). Although advanced CT and MRI technologies exhibit good diagnostic performance for parietal pleural or chest wall invasion, they are relatively expensive, cumbersome, and—in the case of CT scans—emit radiation. In contrast, ultrasonography offers advantages in terms of cost-effectiveness and real-time evaluation of relative movement. Historically, ultrasound was perceived to be less efficacious in evaluating lesions within the lung due to alveolar gas interference. However, subpleural lesions in peripheral lung cancer invasion can be clearly detected by ultrasound without such interference. Thus, ultrasonography may be an effective method for evaluating the parietal pleural adhesion/invasion of subpleural lung cancer.

B-mode ultrasonography has demonstrated superior accuracy in assessing the chest wall invasion of lung cancer compared to traditional CT (13,14). However, this invasion is a type of deep parietal pleural invasion. Lesion mobility and direct signs of invasion in cases of extensive and deep parietal pleural invasion may be obvious and easy to detect; however, early superficial adhesion/invasion may not significantly affect lung lesion mobility, and signs of direct invasion may be occult. Therefore, a more accurate imaging technique is necessary to evaluate the parietal pleural adhesion/invasion of lung cancer, especially for early invasion. Contrast-enhanced ultrasound (CEUS) presents superior contrast compared to two-dimensional ultrasound and provides real-time visualization of microvessel distribution in tissues (15,16). CEUS also overcomes the disadvantage of respiratory motion artifacts when observing blood perfusion. CEUS has been reported to have high accuracy in evaluating the degree of capsular invasion and peripheral tissue infiltration of thyroid cancer, cervical canal cancer, and other organ tumors (17-19). However, its value in evaluating parietal pleural invasion of peripheral lung cancer remains uncertain.

The VX2 tumor originates from squamous cell carcinoma derived from rabbit papilloma induced by the Shope virus. It exhibits characteristics such as implantation feasibility in multiple sites, high survival rate after implantation, and rapid growth. The construction of a rabbit lung cancer animal model using the VX2 tumor has been widely reported for establishing lung cancer patterns and for conducting imaging studies of lung cancer (20-22). This study aimed to investigate the value of B-mode ultrasound and CEUS in

diagnosing parietal pleural adhesion/invasion of subpleural lung cancer in a rabbit lung VX2 tumor model. We present this article in accordance with the STARD reporting checklist (available at https://qims.amegroups.com/article/view/10.21037/qims-23-1542/rc).

Methods

Animals and ethical considerations

The study was approved by the Animal Ethics and Welfare Committee of Southern Medical University (No. NFYY-2021-0339) in compliance with the institution's guidelines for the care and use of animals. The study included 40 male New Zealand white rabbits (Southern Medical University, Guangzhou, Guangdong, China), with an average body weight of 2.5–3.0 kg and aged between 3 and 4 months. Each rabbit was housed individually in cages maintained at a temperature of 16–25 ℃ and humidity of 40–70%. Rabbits, housing, and experimental environments were specific pathogen free. Rabbits were housed in air-conditioned cages with ad libitum access to laboratory food and drinking water, with regular cleaning being conducted. After 2 weeks of domestication, all the rabbits remained healthy.

Preparation of tumor-bearing rabbits

The VX2 tumor tissue, provided by the Experimental Animal Center of Southern Medical University, was dissected using ophthalmic scissors and inoculated into the lateral muscle of the proximal thigh via syringes. One-week postinjection, tumor formation at the injection site was examined via Doppler ultrasound. Successful formation of the VX2 tumor tissue was confirmed through the detection of blood supply at the injection site. Once the tumor reached a size of 1 cm, the tumor tissues were extracted and used to construct the lung cancer model.

Model construction and confirmation of subpleural lung tumors

The objective of this study was to develop an animal model with peripheral lung lesions involving pleural contact, specifically a model of subpleural lung cancer with early parietal pleural invasion. If the injection site were far from the pleura, a large tumor lesion and long growth period would be required to meet the model criteria. However, if the lesions were too large or had a prolonged growth period, this would likely weaken the rabbits, thus making anesthetic procedures and ultrasound examination difficult. Overall, the injection point should be located in the lung parenchyma as close as possible to the parietal pleura. This study adopted ultrasound-guided tumor injection to meet the modeling requirements. The details of the procedure were as follows.

Following anesthesia induction, the left or right chest was randomly selected, with the injection area being as distant as possible from the heart. Skin preparation and routine disinfection were performed on the chest of the target area. A syringe containing 1–2 mL of VX2 tumor tissue block suspension was prepared. First, the needle tip was guided to the pleura under real-time ultrasonic guidance. Subsequently, the needle was advanced 3–5 mm into the subpleural lung parenchyma, and the VX2 tumor tissue was immediately injected (see *Figure 1*). Postinjection complications, such as pneumothorax, hemothorax, or bleeding, were examined with ultrasound. Routine intramuscular injection of 200,000 U/d of penicillin was administered for 1-day postoperation to prevent pulmonary infection. Detailed chest ultrasonography was performed 7 days after tumor implantation. The model was considered to be successfully established if a subpleural lung tumor was detected by ultrasound in the injection area.

Evaluation of subpleural lung lesions and parietal pleural adhesion/invasion

Within 1–3 weeks following subpleural lesion formation, parietal pleural invasion of the largest subpleural lesions was evaluated by ultrasound.

After anesthesia induction, the rabbits were positioned laterally. Ultrasonographic evaluation was performed using a transthoracic ultrasound instrument (Resona 7T; Mindray, Shenzhen, China) with an L9-3U probe (2.5–9.0 MHz). Lung lesions and pleura were evaluated via B-mode ultrasound and CEUS. A sonographer (sonographer 1) with 5 years of experience in chest ultrasound and CEUS performed the ultrasonography and collected lesion data. B-mode ultrasound scanning progress was recorded and stored intermittently. A 0.5 mL/kg bolus of contrast agent (Sonovue; Bracco, Milan, Italy) was then intravenously injected and was followed by a 5.0-mL saline flush. Subsequently, the area was continuously observed for 180 seconds. To test the interrater reliability, another sonographer (sonographer 2) who was blinded to the

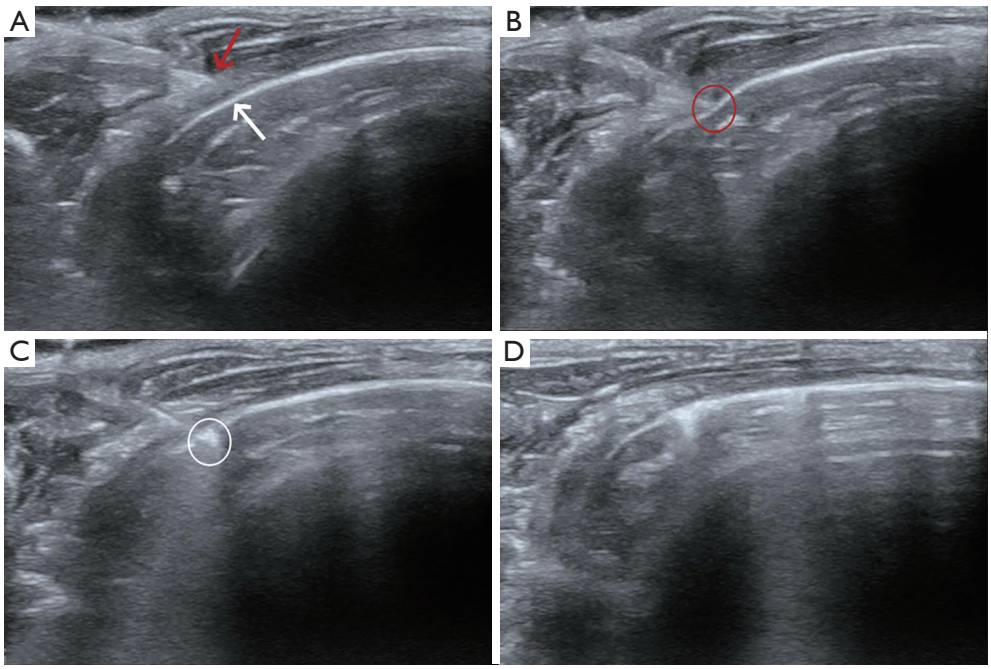

Figure 1 Construction of the rabbit subpleural lung tumor model via injection VX2 tumor tissue under ultrasonic guidance. (A) The needle tip reaches the chest wall under real-time ultrasound guidance but does not touch the pleura (red arrow: needle tip; white arrow: pleura). (B) The needle tip reaches the pleura under real-time ultrasonic guidance (red circle: the point where the needle tip touches the pleura). (C) The needle tip pierces the pleura and penetrates 3–5 mm into the lung parenchyma; echogenic changes appear the pleuropneumonic interface (white circle). (D) No pneumothorax or hemothorax is detected by ultrasound after puncture.

assessment made by sonographer 1 and who had 5 years of experience in chest ultrasound and CEUS reviewed the stored ultrasound scanning video.

Characteristics observed via B-mode ultrasound included the lesion size, presence of pleural effusion, relative movement between subpleural lesions and the chest wall, and communication region between the lesion and the parietal pleura. Lesion size was determined by measuring the maximum diameter of the lesion on ultrasound. As the movement of the lesion could be affected by the respiratory state of the rabbit, the movement was only used as an indicator of suitability for CEUS and not as a standard to confirm whether the lesion was adhesive or invasive. Analysis of adhesion/invasion via B-mode ultrasound analysis of was mainly conducted by observing whether there was an adhesion/invasion zone between the lesion and the parietal pleura. A contiguous band between the two indicated adhesion/invasion; while a mass and a parietal pleura that were smooth and not clearly connected indicated noninvasion.

Characteristics observed via CEUS included the continuity of the parietal pleura, the communication region between the lesion and the parietal pleura, and abnormally enhanced areas between lesions and the parietal pleura. When a connection was found between the mass and the parietal pleura, adhesion/invasion was considered present; otherwise, adhesion/invasion was considered absent.

Diagnostic gold standard of subpleural lesion with parietal pleural adhesion/invasion

The gold standard for detecting parietal pleural adhesion/invasion of subpleural lung cancer is based on anatomical findings during operation and pathological examinations.

Following ultrasound evaluation, the affected disease locations, including the lesion, surrounding lung tissue, and pleura, were anatomically analyzed to ascertain the integrity of the parietal pleura and the presence of adhesions between the parietal pleura and the lesions. Lesions without parietal pleural adhesion/invasion was considered when pleura was smooth and complete without adhesion to the lesion. Conversely, adhesion/invasion of the parietal pleura was confirmed if adhesion was present between the lesion and the parietal pleura upon dissection. When parietal pleural

invasion was suspected and assessment of adhesion/invasion between the lesion and parietal pleura was challenging during the anatomical assessment, a pathological evaluation of the subpleural lesion, visceral pleura, and parietal pleura was conducted for confirmation. All anatomical specimens were fixed in 10% formalin and sent for histopathological examination, which included paraffin-embedding, careful sectioning, and hematoxylin and eosin (HE) staining. All pathological procedures were determined through consultation between two pathologists with at least 5 years of experience who were blinded to the sonographers' evaluation results.

Statistical analyses

Statistical analyses were performed using SPSS version 22.0 (IBM Corp., Armonk, NY, USA). Continuous variables are expressed as the means with standard deviations, and categorical variables are expressed as frequencies or percentages. The accuracy, specificity, and sensitivity of B-mode ultrasound and CEUS in diagnosing parietal pleural adhesion/invasion of subpleural lung cancer by sonographers 1 and 2 were analyzed. The interrater reliability for B-mode ultrasound and CEUS was assessed using weighted kappa statistics. A P value <0.05 in a two-sided test was considered statistically significant.

Results

No immediate pneumothorax or hemorrhage was observed in any rabbit following ultrasound-guided injection. However, three rabbits died under anesthesia before ultrasound evaluation, and an additional three rabbits died during feeding within 1–3 weeks after model construction. Ultimately, 34 rabbits were subjected to complete ultrasonic evaluation. Within 10–14 days after tumor injection, ultrasonography detected subpleural lung cancer in all 34 rabbits (15 left lesions and 19 right lesions), indicating a 100% tumor formation rate. There were 20 and 14 cases of subpleural lesions with and without parietal pleural adhesion/invasion, respectively, confirmed by anatomical and/or pathological assessments. Among the 14 cases without adhesion/invasion, lesions were observed on days 7, 14, and 18 after tumor injection in 7, 6, and 1 cases, respectively (see *Figure 2*). Among the 20 cases with adhesion/invasion, parietal pleural adhesion/invasion was observed on days 14, 18, and 21 after tumor injection in 4, 8, and 8 cases, respectively (see *Figure 3*).

B-mode ultrasound examination

Sonographer 1 identified 10 and 24 subpleural lesions with and without parietal pleural adhesion/invasion, respectively, through B-mode ultrasonography. Compared with the gold standard method, sonographer 1 diagnosed 24 cases correctly and 10 cases incorrectly, all of which were false negatives. The sensitivity, specificity, and accuracy of sonographer 1 using B-mode ultrasound were 50.0% [95% confidence interval (CI): 26.0–74.0%], 100.0%, and 70.6% (95% CI: 54.5–86.7%), respectively (see *Table 1*). Sonographer 2 identified 10 and 24 subpleural lesions with and without parietal pleural adhesion/invasion, respectively, through B-mode ultrasonography. Compared with the gold standard method, sonographer 2 diagnosed 22 cases correctly and 12 cases incorrectly. Of the latter, there was 1 false positive and 11 false negatives. The sensitivity, specificity, and accuracy of sonographer 2 using B-mode ultrasound were 45.0% (95% CI: 21.1–68.9%), 92.9% (95% CI: 77.5–100.0%), and 64.7% (95% CI: 47.8–81.6%), respectively (see *Table 1*).

CEUS examination

The 34 cases of subpleural lesions were unevenly enhanced in CEUS. Sonographer 1 identified 18 and 16 cases of subpleural lesions with and without parietal pleural adhesion/invasion, respectively, through CEUS. Compared with the gold standard method, sonographer 1 correctly diagnosed subpleural lesions with adhesion/invasion in 32 cases and incorrectly in 2 cases. Of the latter, both were false negatives. The sensitivity, specificity, and accuracy of sonographer 1 using CEUS were 90.0% (95% CI: 75.6–100.0%), 100.0%, and 94.1% (95% CI: 85.8–100.0%), respectively (see *Table 1*). Sonographer 2 identified 17 and 17 cases of subpleural lesions with and without parietal pleural adhesion/invasion, respectively, through CEUS. Compared with the gold standard method, sonographer 2 correctly diagnosed subpleural lesions with parietal pleural invasion in 31 cases and incorrectly in 3 cases, all of which were false negatives. The sensitivity, specificity, and accuracy of sonographer 2 using CEUS were 85.0% (95% CI: 67.9–100.0%), 100.0%, and 91.2% (95% CI: 81.1–100.0%), respectively (see *Table 1*).

Comparison of accuracy and interrater reliability between B-mode ultrasound and CEUS

The diagnostic accuracy of sonographer 1 using CEUS

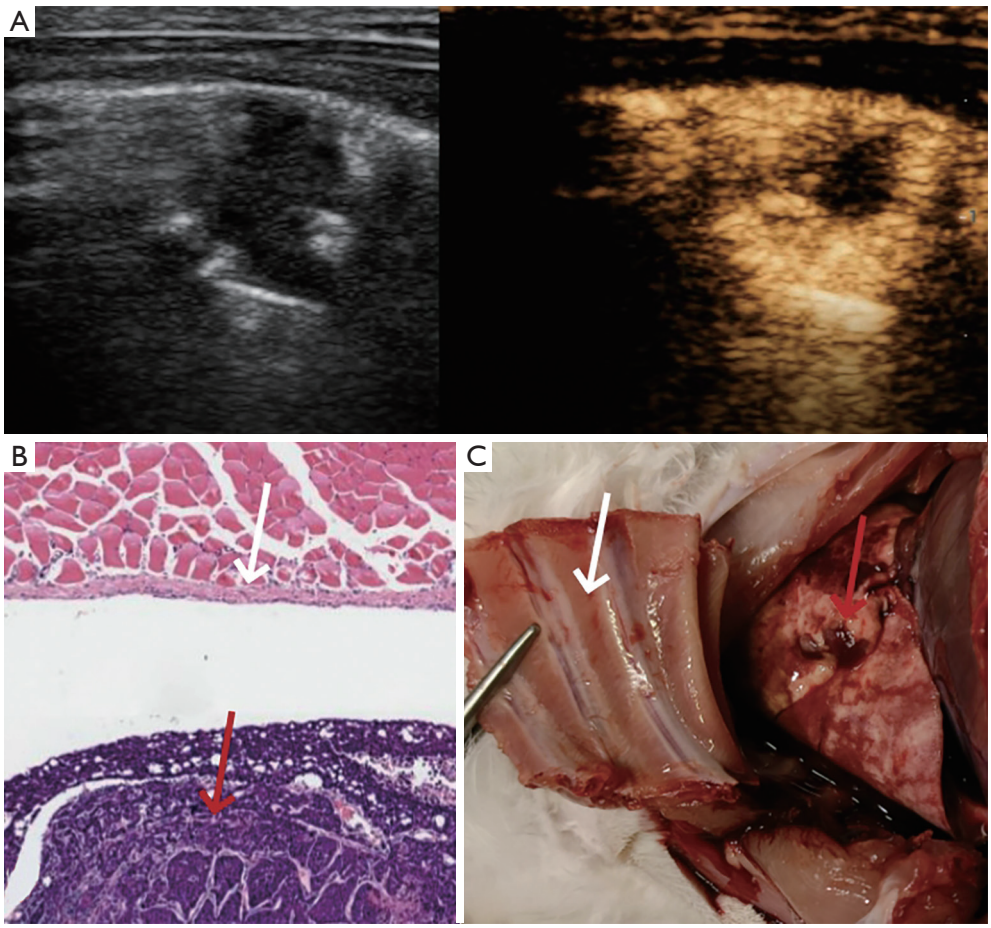

Figure 2 Subpleural lung cancer without parietal pleural adhesion/invasion. (A) B-mode ultrasound and contrast-enhanced ultrasound show the parietal pleura is smooth and complete, with no obvious invasion or adhesion between the lesion and the parietal pleural. (B) Pathology confirms (hematoxylin and eosin staining, ×100) no parietal pleural adhesion/invasion. The red arrow indicates the tumor, and the white arrow indicates the parietal pleura. (C) Dissection confirms no parietal pleural adhesion/invasion. The red arrow indicates the tumor, and the white arrow indicates the parietal pleura.

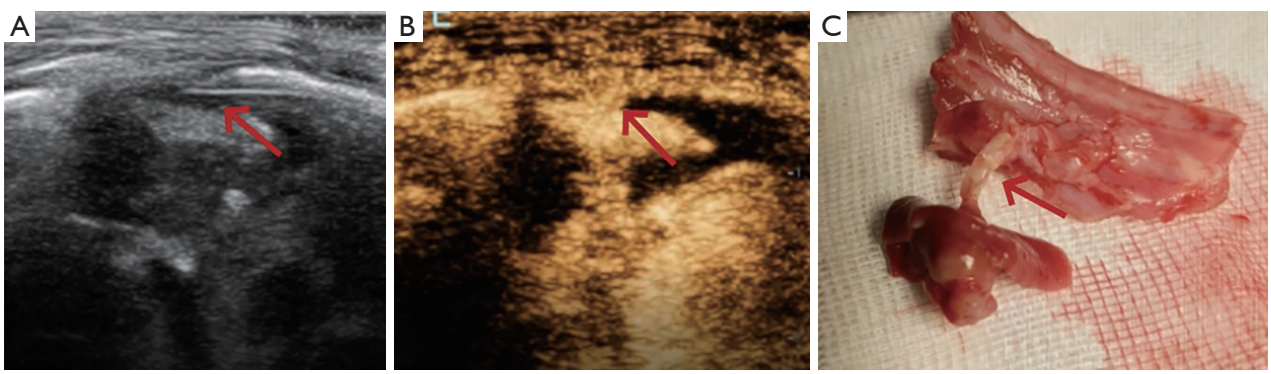

Figure 3 Subpleural lung cancer with early local invasion of the pleura and parietal pleural adhesion/invasion. (A,B) No obvious invasion/adhesion is observed by B-mode ultrasound, while invasion/adhesion between the lesion and parietal pleural is detected by contrast-enhanced ultrasound (red arrow). (C) Invasion/adhesion between the lesion and parietal pleura is also found during dissection (red arrow).

Table 1 The accuracy of the two sonographers in evaluating parietal pleural adhesion/invasion using and CEUS and B-mode ultrasound

Evaluator	Ultrasound diagnosis	Dissection and/or pathology, number		Accuracy (95% CI)
		Adhesion/invasion (20)	No adhesion/invasion (14)	
Sonographer 1	B-mode ultrasound	–	–	70.6% (54.5–86.7%)
	Adhesion/invasion	10	0	–
	No adhesion/invasion	10	14	–
	CEUS	–	–	94.1% (85.8–100.0%)
	Adhesion/invasion	18	0	–
	No adhesion/invasion	2	14	–
Sonographer 2	B-mode ultrasound	–	–	64.7% (47.8–81.6%)
	Adhesion/invasion	9	1	–
	No adhesion/invasion	11	13	–
	CEUS	–	–	91.2% (81.1–100.0%)
	Adhesion/invasion	17	0	–
	No adhesion/invasion	3	14	–

CEUS, contrast-enhanced ultrasound; CI, confidence interval.

was not significantly higher than that of using B-mode ultrasound (94.1% *vs.* 70.6%; P=0.08). Meanwhile, the diagnostic accuracy of sonographer 2 using CEUS was significantly higher than that of using B-mode ultrasound (91.2% *vs.* 64.7%; P=0.03). The κ value of interrater reliability between sonographers 1 and 2 was 0.717 for B-mode ultrasound (P<0.001), and the κ value of interrater reliability between sonographers 1 and 2 was deemed to be excellent for CEUS (κ=0.941; P<0.001).

Discussion

Accurate and convenient preoperative diagnostic imaging of parietal pleural adhesion/invasion is important for formulating treatment plans for patients with peripheral lung cancer. To achieve this, we established a novel animal model of subpleural lung cancer with parietal pleural adhesion/invasion through ultrasound-guided injection. Subsequently, we investigated the value of CEUS in evaluating parietal pleural adhesion/invasion of subpleural lung cancer and compared the diagnostic efficacy and interrater reliability of CEUS and B-mode ultrasound.

Previously reported methods for establishing a rabbit VX2 lung tumor model have mainly included blind percutaneous injection, percutaneous CT-guided injection, and transbronchial inoculation (20-22). Blind injection poses challenges in controlling the injection site, and percutaneous CT-guided injection, despite facilitating injection site monitoring, is cumbersome, radioactive, and relatively expensive. Transbronchial inoculation presents difficulty in injecting tumor tissues into the subpleural bronchioles and is highly dependent on the operator's skill and experience. Considering the advantages of real-time ultrasonography, including convenience, absence of radiation exposure, and low cost, we attempted to establish an animal model using percutaneous ultrasound-guided injection. The needle tip was directed to the pleura under ultrasonic guidance and tumor tissues were immediately injected, ensuring precise injection as close to the pleura as possible (see *Figure 1*). This novel approach to constructing a subpleural lung tumor model through ultrasound-guided tumor injection provides a new animal model of lung tumors and may be beneficial for subsequent research.

Ultrasonography cannot discover lesions within the lung due to interference of lung gases, leading to its underutilization in diagnosing thoracic tumors. However, the chest wall, pleura, and subpleural lung tumors are not impacted by lung gases, and their locations are shallow (see *Figure 2*). Therefore, the association between subpleural lung cancer and the parietal pleura, such as adhesion/invasion, can be investigated by ultrasound. Researchers have reported B-mode ultrasound to be more accurate than CT in diagnosing wall invasion of lung cancer, possibly because ultrasound allows for real-time evaluation of

a lesion's movement (13,14). The weakness in relative movement between lung lesions and the parietal pleura or chest wall is an important imaging feature for diagnosing parietal pleural adhesion/invasion, whether by ultrasound, four-dimensional dynamic-ventilation CT, or dynamic MRI (10-14). However, chest wall invasion represents deep parietal pleural invasion. It remains uncertain whether such weak movement can help diagnose early local parietal pleural adhesion/invasion. In the early parietal pleural adhesion/invasion animal model developed in this study, there was a tendency toward weaker movement in cases involving large-scale or deep invasion. However, such movement may not necessarily be significantly weakened in slight local or early-stage parietal pleural adhesion/invasion. Therefore, in addition to examining lesion movement, observing areas of adhesion/invasion is also critical. In our study, we used continuity of the parietal pleura and communication between lesions and the parietal pleura to determine the accuracy of B-mode ultrasound in diagnosing parietal pleural adhesion/invasion of subpleural lung cancer, ultimately yielding an accuracy of 70.6%, which is slightly lower than previously reported rates. This is likely due to the prevalence of early local parietal pleural invasion in our cases (13,14).

Although B-mode ultrasound has acceptable diagnostic efficacy in diagnosing parietal pleural adhesion/invasion of subpleural lung cancer, employing advanced ultrasound technologies may further improve the diagnostic value of ultrasonography. With the increasing recognition and application of thoracic ultrasound, the value of CEUS in diagnosing lung and pleural diseases has attracted greater attention. CEUS can differentiate benign from malignant lung lesions and lung cancer with pneumonia (22-24). CEUS also has good diagnostic efficacy in differentiating benign from malignant pleural diseases (25,26). However, its value in diagnosing parietal pleural invasion of subpleural lung cancer remains uncertain. This is the first study to investigate the value of CEUS value in evaluating parietal pleural adhesion/invasion of subpleural lung cancer, revealing a sensitivity, specificity, and accuracy of 90.0%, 100.0%, and 94.1%, respectively. We also demonstrated that the accuracy of CEUS was significantly better than that of B-mode ultrasound. One study reported that CEUS is a more valuable noninvasive imaging technique than is B-mode ultrasound for detecting extracapsular extension of papillary thyroid cancer due to its ability to detect abnormal microvascular perfusion at the invasion area (17). The formation of adhesion/invasion is based on the formation of abnormal microcirculation whether in the early or progressive stages. CEUS is convenient and can be performed in real time, and it has high sensitivity in detecting microvascular perfusion. Additionally, CEUS can observe the relative movement between the lesion and chest wall and can also identify areas of early-stage adhesion/invasion, unlike B-mode ultrasound (see *Figure 3*). Overall, CEUS exhibited excellent diagnostic ability in evaluating parietal pleural invasion of subpleural lung cancer, especially early-stage invasion.

We also investigated the interrater reliability of CEUS and B-mode ultrasound in diagnosing parietal pleural adhesion/invasion of subpleural lung cancer; in addition to diagnostic accuracy, this metric is also an important indicator of the clinical applicability of ultrasonography, especially in emerging fields. CEUS has exhibited excellent interrater reliability in evaluating lesion size and enhancement mode, as well as in identifying inferior vena cava wall invasion (κ=0.90) and differentiating bland thrombus from tumor thrombus (κ=0.97) (27-29). In our study, we found that CEUS and B-mode ultrasound had satisfactory interrater reliability in evaluating parietal pleural adhesion/invasion, but CEUS was superior to B-mode ultrasound (κ=0.941 *vs.* κ=0.717).

This study has some limitations. First, an animal model was employed, so further clinical verification is required. Second, due to experimental constraints, ultrasonography was not compared with CT or MRI. Furthermore, adhesion and invasion were not subdivided in this study. Finally, due to limited sample sizes, we could not analyze the factors influencing diagnostic accuracy.

Conclusions

Based on an animal model, B-mode ultrasound and CEUS exhibited good diagnostic efficacy and interrater reliability in evaluating parietal pleural adhesion/invasion of subpleural lung cancer, with CEUS showing superiority in both metrics.

Acknowledgments

Funding: This work was supported by the Science and Technology Program of Guangzhou, China (No. 202201020433); the Medical Scientific Research Foundation of Guangdong Province, China (No. A2020408); the Project of Guangzhou Municipal Health Bureau, China (No. 20231A011085); and the Key R&D Plan of the Ministry of Science and Technology, China (No. 2023YFC2411700).

Footnote

Reporting Checklist: The authors have completed the STARD reporting checklist. Available at https://qims.amegroups.com/article/view/10.21037/qims-23-1542/rc

Conflicts of Interest: All authors have completed the ICMJE uniform disclosure form (available at https://qims.amegroups.com/article/view/10.21037/qims-23-1542/coif). The authors have no conflicts of interest to declare.

Ethical Statement: The authors are accountable for all aspects of the work in ensuring that questions related to the accuracy or integrity of any part of the work are appropriately investigated and resolved. The study was approved by the Animal Ethics and Welfare Committee of Southern Medical University (No. NFYY-2021-0339) in compliance with the institution's guidelines for the care and use of animals.

References

1. Ferlay J, Colombet M, Soerjomataram I, Mathers C, Parkin DM, Piñeros M, Znaor A, Bray F. Estimating the global cancer incidence and mortality in 2018: GLOBOCAN sources and methods. Int J Cancer 2019;144:1941-53.
2. Goldstraw P, Chansky K, Crowley J, Rami-Porta R, Asamura H, Eberhardt WE, Nicholson AG, Groome P, Mitchell A, Bolejack V; International Association for the Study of Lung Cancer Staging and Prognostic Factors Committee, Advisory Boards, and Participating Institutions; International Association for the Study of Lung Cancer Staging and Prognostic Factors Committee Advisory Boards and Participating Institutions. The IASLC Lung Cancer Staging Project: Proposals for Revision of the TNM Stage Groupings in the Forthcoming (Eighth) Edition of the TNM Classification for Lung Cancer. J Thorac Oncol 2016;11:39-51.
3. Eberhardt WE, Mitchell A, Crowley J, Kondo H, Kim YT, Turrisi A 3rd, Goldstraw P, Rami-Porta R; International Association for Study of Lung Cancer Staging and Prognostic Factors Committee, Advisory Board Members, and Participating Institutions. The IASLC Lung Cancer Staging Project: Proposals for the Revision of the M Descriptors in the Forthcoming Eighth Edition of the TNM Classification of Lung Cancer. J Thorac Oncol 2015;10:1515-22.
4. Yip R, Ma T, Flores RM, Yankelevitz D, Henschke CI; International Early Lung Cancer Action Program Investigators. Survival with Parenchymal and Pleural Invasion of Non-Small Cell Lung Cancers Less than 30 mm. J Thorac Oncol 2019;14:890-902.
5. Postmus PE, Brambilla E, Chansky K, Crowley J, Goldstraw P, Patz EF Jr, Yokomise H; International Association for the Study of Lung Cancer International Staging Committee; Cancer Research and Biostatistics; Observers to the Committee; Participating Institutions. The IASLC Lung Cancer Staging Project: proposals for revision of the M descriptors in the forthcoming (seventh) edition of the TNM classification of lung cancer. J Thorac Oncol 2007;2:686-93.
6. Kawaguchi K, Mori S, Usami N, Fukui T, Mitsudomi T, Yokoi K. Preoperative evaluation of the depth of chest wall invasion and the extent of combined resections in lung cancer patients. Lung Cancer 2009;64:41-4.
7. Satoh Y, Ishikawa Y, Inamura K, Okumura S, Nakagawa K, Tsuchiya E. Classification of parietal pleural invasion at adhesion sites with surgical specimens of lung cancer and implications for prognosis. Virchows Arch 2005;447:984-9.
8. Tanju S, Erus S, Selçukbiricik F, İliaz S, Kapdağlı M, Bulutay P, Sevinç TE, Mandel NM, Dilege Ş. Level of pleural invasion effects on prognosis in lung cancer. Tumori 2019;105:155-60.
9. Mikubo M, Nakashima H, Naito M, Matsui Y, Shiomi K, Jiang SX, Satoh Y. Prognostic impact of uncertain parietal pleural invasion at adhesion sites in non-small cell lung cancer patients. Lung Cancer 2017;108:103-8.
10. Yamashiro T, Moriya H, Tsubakimoto M, Nagatani Y, Kimoto T, Murayama S; . Preoperative assessment of parietal pleural invasion/adhesion of subpleural lung cancer: advantage of software-assisted analysis of 4-dimensional dynamic-ventilation computed tomography. Eur Radiol 2019;29:5247-52.
11. Akata S, Kajiwara N, Park J, Yoshimura M, Kakizaki D, Abe K, Hirano T, Ohira T, Tsuboi M, Kato H. Evaluation

of chest wall invasion by lung cancer using respiratory dynamic MRI. J Med Imaging Radiat Oncol 2008;52:36-9.
12. Sakuma K, Yamashiro T, Moriya H, Murayama S, Ito H. Parietal pleural invasion/adhesion of subpleural lung cancer: Quantitative 4-dimensional CT analysis using dynamic-ventilatory scanning. Eur J Radiol 2017;87:36-44.
13. Bandi V, Lunn W, Ernst A, Eberhardt R, Hoffmann H, Herth FJ. Ultrasound vs. CT in detecting chest wall invasion by tumor: a prospective study. Chest 2008;133:881-6.
14. Tahiri M, Khereba M, Thiffault V, Ferraro P, Duranceau A, Martin J, Liberman M. Preoperative assessment of chest wall invasion in non-small cell lung cancer using surgeon-performed ultrasound. Ann Thorac Surg 2014;98:984-9.
15. Dietrich CF, Nolsøe CP, Barr RG, Berzigotti A, Burns PN, Cantisani V, et al. Guidelines and Good Clinical Practice Recommendations for Contrast Enhanced Ultrasound (CEUS) in the Liver - Update 2020 - WFUMB in Cooperation with EFSUMB, AFSUMB, AIUM, and FLAUS. Ultraschall Med 2020;41:562-85.
16. Sidhu PS, Cantisani V, Dietrich CF, Gilja OH, Saftoiu A, Bartels E, et al. The EFSUMB Guidelines and Recommendations for the Clinical Practice of Contrast-Enhanced Ultrasound (CEUS) in Non-Hepatic Applications: Update 2017 (Long Version). Ultraschall Med 2018;39:e2-e44.
17. Zhang Y, Zhang X, Li J, Cai Q, Qiao Z, Luo YK. Contrast-enhanced ultrasound: a valuable modality for extracapsular extension assessment in papillary thyroid cancer. Eur Radiol 2021;31:4568-75.
18. Wu M, Wu J, Huang L, Chen Y, Qu E, Xu J, Kuang X, Zhang X. Comparison of contrast-enhanced ultrasonography and magnetic resonance imaging in the evaluation of tumor size and local invasion of surgically treated cervical cancer. Abdom Radiol (NY) 2022;47:2928-36.
19. Xiao Y, Xu D, Ju H, Yang C, Wang L, Wang J, Hazle JD, Wang D. Application value of biplane transrectal ultrasonography plus ultrasonic elastosonography and contrast-enhanced ultrasonography in preoperative T staging after neoadjuvant chemoradiotherapy for rectal cancer. Eur J Radiol 2018;104:20-5.
20. Ueki A, Okuma T, Hamamoto S, Miki Y. Therapeutic Effects of CT-guided Radiofrequency Ablation with Concurrent Platinum-Doublet Chemotherapy in a Rabbit VX2 Lung Tumor Model. Radiology 2017;283:391-8.
21. Kinoshita T, Effat A, Gregor A, Inage T, Ishiwata T, Motooka Y, Ujiie H, Wilson BC, Zheng G, Weersink R, Asamura H, Yasufuku K. A Novel Laser Fiberscope for Simultaneous Imaging and Phototherapy of Peripheral Lung Cancer. Chest 2019;156:571-8.
22. Xing J, He W, Ding YW, Li Y, Li YD. Correlation between Contrast-Enhanced Ultrasound and Microvessel Density via CD31 and CD34 in a rabbit VX2 lung peripheral tumor model. Med Ultrason 2018;1:37-42.
23. Bi K, Zhou RR, Zhang Y, Shen MJ, Chen HW, Cong Y, Zhu HM, Tang CH, Yuan J, Wang Y. US Contrast Agent Arrival Time Difference Ratio for Benign versus Malignant Subpleural Pulmonary Lesions. Radiology 2021;301:200-10.
24. Fu Y, Lei Y, Cui L, Du T, Mei F. Can Ultrasound and Contrast-Enhanced Ultrasound Help Differentiate between Subpleural Focal Organizing Pneumonia and Primary Lung Malignancy? Diagnostics (Basel) 2022;12:2074.
25. Findeisen H, Görg C, Hartbrich R, Dietrich CF, Görg K, Trenker C, Safai Zadeh E. Contrast-enhanced ultrasound is helpful for differentiating benign from malignant parietal pleural lesions. J Clin Ultrasound 2022;50:90-8.
26. Safai Zadeh E, Weide J, Dietrich CF, Trenker C, Koczulla AR, Görg C. Diagnostic Accuracy of B-Mode- and Contrast-Enhanced Ultrasound in Differentiating Malignant from Benign Pleural Effusions. Diagnostics (Basel) 2021;11:1293.
27. Li W, Li L, Zhuang BW, Ruan SM, Hu HT, Huang Y, Lin MX, Xie XY, Kuang M, Lu MD, Chen LD, Wang W. Inter-reader agreement of CEUS LI-RADS among radiologists with different levels of experience. Eur Radiol 2021;31:6758-67.
28. Yan L, Luo Y, Xiao J, Lin L. Non-enhanced ultrasound is not a satisfactory modality for measuring necrotic ablated volume after radiofrequency ablation of benign thyroid nodules: a comparison with contrast-enhanced ultrasound. Eur Radiol 2021;31:3226-36.
29. Li QY, Li N, Huang QB, Luo YK, Wang BJ, Guo AT, Ma X, Zhang X, Tang J. Contrast-enhanced ultrasound in detecting wall invasion and differentiating bland from tumor thrombus during robot-assisted inferior vena cava thrombectomy for renal cell carcinoma. Cancer Imaging 2019;19:79.

Cite this article as: Zhang Y, Zhang Z, Liao H, Li M, Xu C, Liang Z, He L, Zhang S, Tang Q. Evaluation of parietal pleural adhesion and invasion in subpleural lung cancer: value of B-mode ultrasound and contrast-enhanced ultrasound. Quant Imaging Med Surg 2024;14(5):3302-3311. doi: 10.21037/qims-23-1542

